

A possible giant planet orbiting the cataclysmic variable LX Ser

Li K.^{1,2}, Hu, S.-M.¹, Zhou, J.-L.³, Wu, D.-H.³, Guo, D.-F.¹, Jiang, Y.-G.¹, Gao, D.-Y.¹, Chen, X.¹, Wang, X.-Y.¹

ABSTRACT

LX Ser is a deeply eclipsing cataclysmic variable with an orbital period of $0.^d1584325$. Sixty two new eclipse times were determined by our observations and the AAVSO International Data base. Combining all available eclipse times, we analyzed the $O - C$ behavior of LX Ser. We found that the $O - C$ diagram of LX Ser shows a sinusoidal oscillation with a period of 22.8 yr and an amplitude of 0.00035 days. Two mechanisms (i.e., the Applegate mechanism and the light travel time effect) are applied to explain the cyclic modulation. We found that the Applegate mechanism is difficult to explain the cyclic oscillation in the orbital period. Therefore, the cyclic period change is most likely to be caused by the light travel time effect due to the presence of a third body. The mass of the tertiary component was determined to be $M_3 \sim 7.5 M_{Jup}$. We supposed that the tertiary companion is plausible a giant planet. The stability of the giant planet was checked, and we found that the multiple system is stable.

Subject headings: stars: binaries: eclipsing — stars: novae, cataclysmic variables — stars: individual (LX Ser)

1. Introduction

Cataclysmic variables (CVs) are interacting binary stars composed of a degenerate white dwarf primary and a Roche lobe filling M dwarf secondary. LX Ser was first identified to be an eclipsing CV by Stepanian (1979) when searching galaxies with ultraviolet continuum and

¹Shandong Provincial Key Laboratory of Optical Astronomy and Solar-Terrestrial Environment, Institute of Space Sciences, Shandong University, Weihai, 264209, China (e-mail: kaili@sdu.edu.cn, likai@ynao.ac.cn (Li, K.), husm@sdu.edu.cn (Hu, S.-M.))

²Key Laboratory for the Structure and Evolution of Celestial Objects, Chinese Academy of Sciences, Kunming 650011, China

³School of Astronomy and Space Science and Key Laboratory of Modern Astronomy and Astrophysics in Ministry of Education, Nanjing University, Nanjing 210093, China

was classified to be SW Sex subclass of CVs. Stepanian (1979) found that the brightness of LX Ser was about $m_V = 14$ mag. Recently, the orbital inclination and mass ratio of LX Ser were determined to be $i = 79^\circ.0$ and $q = 0.50$ by Marin et al. (2007). By analyzing the eclipse times of LX Ser, Horne (1980) determined an ephemeris $HJD = 2444293.02377(\pm 0.00020) + 0^d.1584328(\pm 0.0000010)E$ and showed that an upper limit on \dot{P} is 10^{-5} . Eason et al. (1984) derived a new ephemeris using a second-order least-squares fitting of all the eclipse times, and the second-order term was insignificant and was ignored. After that, many new eclipse times were obtained (e.g., Agerer & Hubscher 2003; Diethelm 2003; Zejda 2004; Hubscher et al. 2005; Krajci 2005, 2006; Zejda et al. 2006), allowing us to reanalyze the eclipse times.

Eclipsing times of CVs can be determined with high precision, and small amplitude orbital period changes could be discovered. Therefore, CVs are very good targets to search for planetary-mass companions. The presence of the planetary companions orbiting the central stars will cause small wobbles of the barycenter of the triple system. The light from the stars will travel closer or further due to the variation of the distance between the host system and the earth. Then, the arrival eclipse times vary cyclically and the observed-calculated ($O - C$) diagram shows a cyclic change. By analyzing the $O - C$ variations, very small mass companions can be detected. This method has been successfully used to detect substellar companions surrounding CVs, e.g., Z Cha (Dai et al. 2009), DP Leo (Qian et al. 2010a), QS Vir (Qian et al. 2010b), UZ For (Potter et al. 2011), V2051 Oph (Qian et al. 2015). In this paper, we show the investigation of the eclipse times of LX Ser and the possible giant planet orbiting this system.

2. New Observations

New photometric observations of LX Ser were carried out on April 24, May 30, and June 26, 2015, and February 20, 2016. The CCD images were taken by using the 1.0 m Cassegrain telescope at Weihai Observatory of Shandong University (Hu et al. 2014) with the Andor DZ936 camera. The size of each pixel is $0.35''$, resulting that the effective field of view is about $11.8' \times 11.8'$. The observation information is listed in Table 1. All the CCD images were analyzed using the IMRED and PHOT packages in IRAF¹ procedure. The light curve in R_c band observed on April 24, 2015 is displayed in Figure 1 for example. The brightness flickering outside the eclipse can be seen, which is caused by variations of mass transfer rate from the secondary red dwarf to the primary white dwarf. Four new times of

¹IRAF is distributed by the National Optical Astronomy Observatories, which is operated by the Association of Universities for Research in Astronomy Inc., under contract to the National Science Foundation.

light minimum were determined and are shown in Table 2. Our new eclipse times are 3 or 4 significant figures, indicating very high precision. We also collected the data from AAVSO (American Association of Variable Stars Observers) International Data base¹. Based on the data, 58 eclipse times were reanalyzed and are also listed in Table 2, the corresponding light curves are displayed in Figure 2. All the eclipse times were determined by this work using the parabolic fitting method and was converted to Barycentric Julian Dates (BJD) using the software of Eastman et al. (2010). As seen in Figures 1 and 2, all the eclipse times can be fitted by parabolic curves very well.

3. Investigation of the $O - C$ diagram

Since the discovery, LX Ser has been continuously monitored. Many highly precise eclipse times were determined. All the eclipse times collected from literatures including our 62 new determined ones are listed in Table 3. The eclipse times collected from literatures are checked again since some data were derived a long time ago and obtained by different observatories or filters. Those having obviously erring are abandoned. Some of the eclipse times were not given errors in the literatures. The errors of the visual data are assumed to be 0.00100, while that of the photoelectric and CCD data are 0.00010. We constructed the $O - C$ diagram using the following linear ephemeris taken from O-C Gateway² (the initial epoch was converted to BJD),

$$Min.I = BJD2444293.02457 + 0^d.1584325E. \quad (1)$$

The $O - C$ values are listed in Table 3 and the corresponding $O - C$ curve is plotted in the upper panel of Figure 3. A linear function was used to fit the $O - C$ values. By using the

¹<http://www.aavso.org/>

²<http://var2.astro.cz/ocgate/>

Table 1: Observation information of LX Ser

Date	Duration time (hr)	Filter	Exposure time (s)
24 Apr., 2015	3.89	R _c	100
30 May, 2015	0.78	R _c	100
26 Jun., 2015	0.65	V	100
20 Feb., 2016	0.94	N ¹	30

¹ N means no filter.

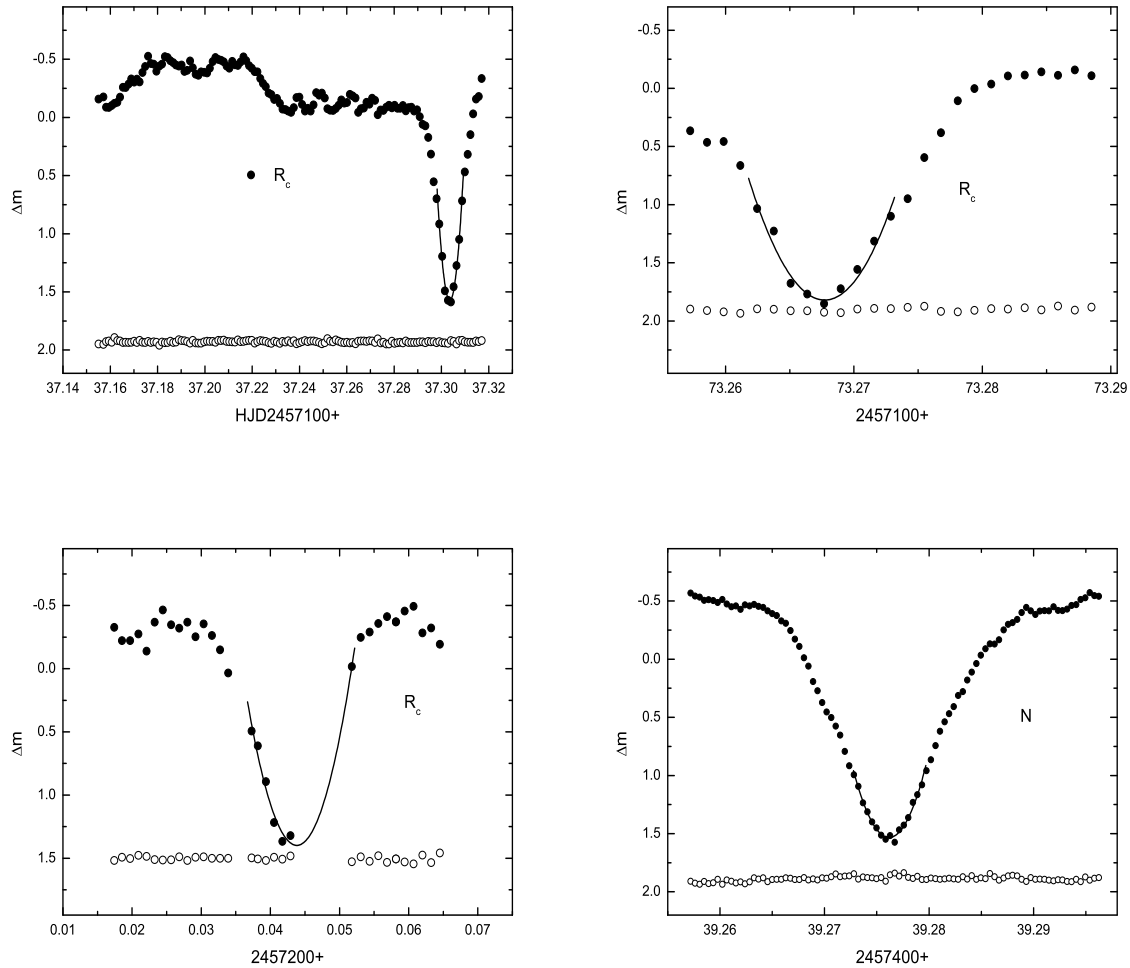


Fig. 1.— The light curves of LX Ser observed using the 1.0 m Cassegrain telescope at Weihai Observatory of Shandong University. The solid and open circles represent magnitude differences between LX Ser and the comparison star and those between the comparison and the check stars, while the solid lines refer to the parabolic fits for the eclipse times.

Table 2: New eclipse times of LX Ser

HJD	BJD	Errors	Cycle	Source	HJD	BJD	Errors	Cycle	Source
2452777.87530	2452777.87605	0.00008	53555	AAVSO	2455672.43733	2455672.43811	0.00016	71825	AAVSO
2452778.82581	2452778.82656	0.00010	53561	AAVSO	2455778.42896	2455778.42974	0.00011	72494	AAVSO
2452779.77639	2452779.77714	0.00008	53567	AAVSO	2456028.43535	2456028.43613	0.00010	74072	AAVSO
2452779.93490	2452779.93565	0.00012	53568	AAVSO	2456088.48114	2456088.48192	0.00009	74451	AAVSO
2452780.72718	2452780.72793	0.00015	53573	AAVSO	2456101.63073	2456101.63151	0.00012	74534	AAVSO
2452780.88538	2452780.88613	0.00013	53574	AAVSO	2456378.88725	2456378.88804	0.00014	76284	AAVSO
2452781.83613	2452781.83688	0.00012	53580	AAVSO	2456381.89715	2456381.89794	0.00019	76303	AAVSO
2452782.78677	2452782.78752	0.00012	53586	AAVSO	2456383.79856	2456383.79935	0.00029	76315	AAVSO
2452782.94532	2452782.94607	0.00013	53587	AAVSO	2456384.43209	2456384.43288	0.00015	76319	AAVSO
2452783.73740	2452783.73815	0.00009	53592	AAVSO	2456384.59069	2456384.59148	0.00015	76320	AAVSO
2452786.74781	2452786.74856	0.00013	53611	AAVSO	2456384.74908	2456384.74987	0.00016	76321	AAVSO
2452786.90609	2452786.90684	0.00009	53612	AAVSO	2456385.85843	2456385.85922	0.00020	76328	AAVSO
2452787.85687	2452787.85762	0.00010	53618	AAVSO	2456386.80920	2456386.80999	0.00017	76334	AAVSO
2453500.48638	2453500.48711	0.00011	58116	AAVSO	2456389.50214	2456389.50293	0.00011	76351	AAVSO
2453502.54540	2453502.54613	0.00031	58129	AAVSO	2456389.66136	2456389.66215	0.00021	76352	AAVSO
2453506.50728	2453506.50801	0.00033	58154	AAVSO	2456403.44384	2456403.44463	0.00008	76439	AAVSO
2453514.42838	2453514.42911	0.00037	58204	AAVSO	2456410.41514	2456410.41593	0.00016	76483	AAVSO
2453516.48800	2453516.48873	0.00035	58217	AAVSO	2456427.68469	2456427.68548	0.00020	76592	AAVSO
2453519.49811	2453519.49884	0.00042	58236	AAVSO	2456782.41510	2456782.41588	0.00006	78831	AAVSO
2453521.39970	2453521.40043	0.00039	58248	AAVSO	2456792.39590	2456792.39668	0.00020	78894	AAVSO
2453521.55769	2453521.55842	0.00040	58249	AAVSO	2456798.41636	2456798.41714	0.00006	78932	AAVSO
2453541.52033	2453541.52106	0.00012	58375	AAVSO	2457091.67550	2457091.67627	0.00007	80783	AAVSO
2454316.41428	2454316.41502	0.00008	63266	AAVSO	2457094.68559	2457094.68636	0.00021	80802	AAVSO
2454580.52079	2454580.52153	0.00034	64933	AAVSO	2457097.69575	2457097.69652	0.00005	80821	AAVSO
2454628.52582	2454628.52656	0.00013	65236	AAVSO	2457134.45164	2457134.45241	0.00004	81053	AAVSO
2454976.44292	2454976.44368	0.00014	67432	AAVSO	2457137.30350	2457137.30427	0.00007	81071	1m
2454994.50413	2454994.50489	0.00006	67546	AAVSO	2457159.48411	2457159.48488	0.00005	81211	AAVSO
2455001.47512	2455001.47588	0.00007	67590	AAVSO	2457163.44506	2457163.44583	0.00013	81236	AAVSO
2455037.43966	2455037.44042	0.00017	67817	AAVSO	2457173.26766	2457173.26843	0.00015	81298	1m
2455662.45633	2455662.45711	0.00016	71762	AAVSO	2457200.04314	2457200.04391	0.00049	81467	1m
2455663.40660	2455663.40738	0.00022	71768	AAVSO	2457439.27695	2457439.27695	0.00004	82977	1m

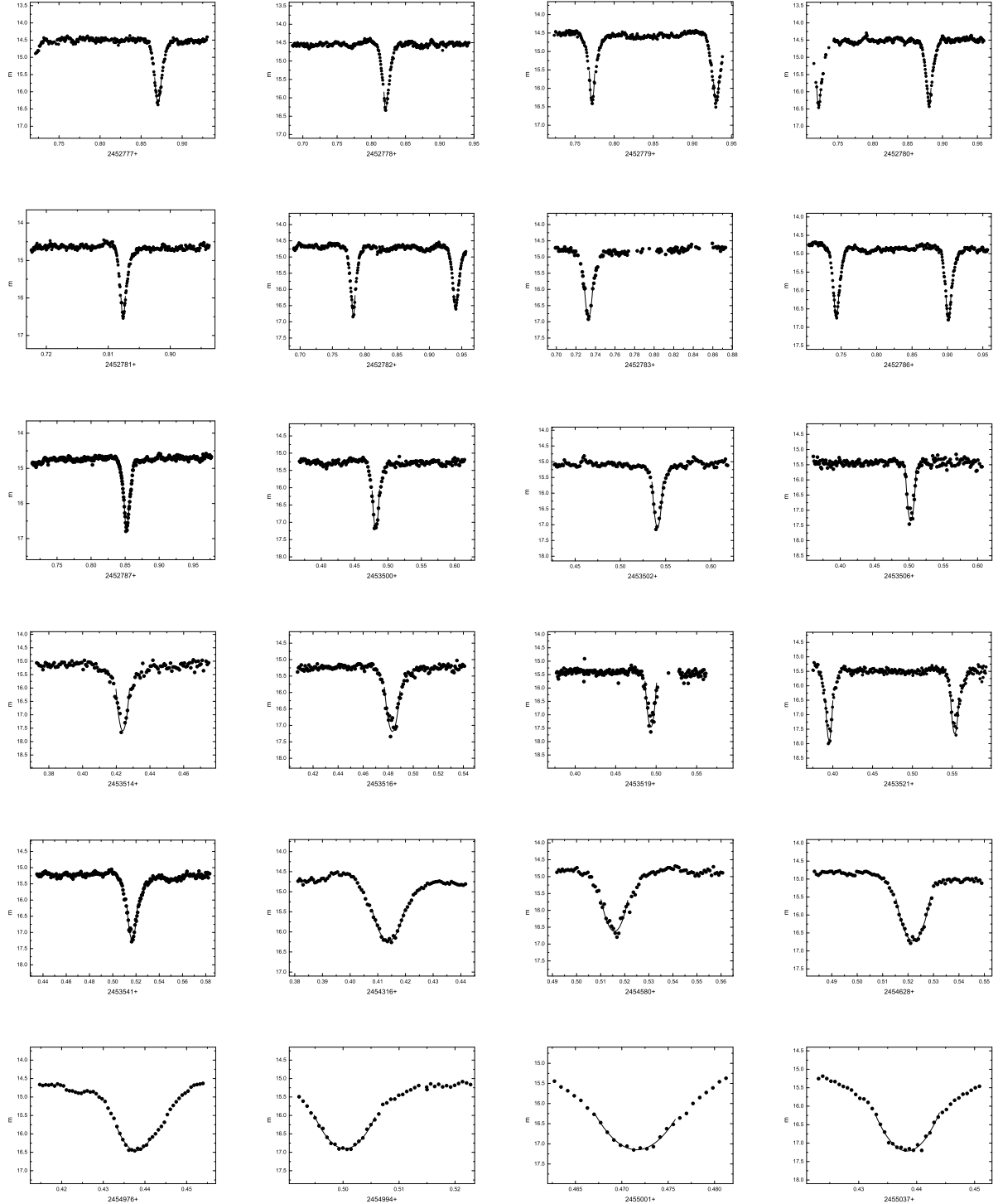


Fig. 2.— The light curves of LX Ser using the AAVSO data. The solid circles represent the visual magnitude of LX Ser, while the solid lines refer to the parabolic fits for the eclipse times.

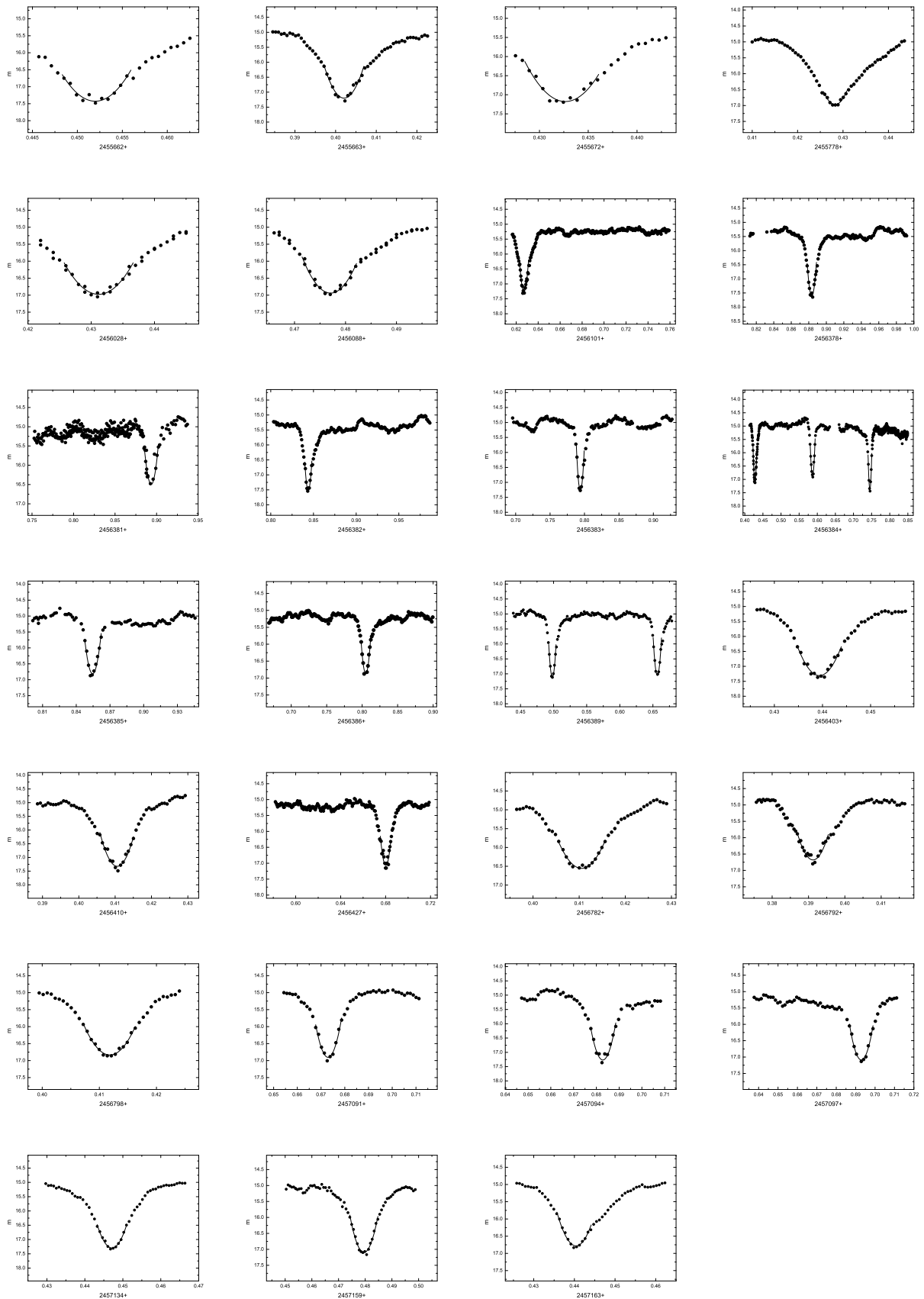


Fig. 2.— continued

weighted least-squares method, we determined the following equation

$$\text{Min.}I = \text{BJD}2444293.024192(\pm 0.000083) + 0^d.158432491(\pm 0.000000002) \times E. \quad (2)$$

The variance is $\sigma_1 = 5.14 \times 10^{-7}$ and the fitting curve is displayed in Figure 3. During the fitting, the weight for the visual data is 1, while that for the photoelectric and CCD data is 10. As seen in the lower panel of Figure 3, a possible small amplitude oscillation can be extracted. Therefore, we intended to use a simultaneous linear-plus-sinusoidal function to fit the $O - C$ curve. In order to determine the period of the sinusoidal variation, the Period04 package (Lenz & Breger 2005) was employed. The resulting Fourier spectrum is shown in Figure 4. A peak at $f = 1.90386493(\pm 0.06022577) \times 10^{-5}$ was obtained, meaning that the period of the sinusoidal variation is $22.80(\pm 0.72)$ yr.

Using the weighted least-squares method, we determined the following equation,

$$\begin{aligned} \text{Min.}I = \text{BJD}2444293.023557(\pm 0.000191) + 0^d.158432495(\pm 0.000000002) \times E + \\ + 0^d.00035(\pm 0.00008) \times \sin [0^\circ.00685 \times E + 32^\circ.8(\pm 0.3)]. \end{aligned} \quad (3)$$

The variance is $\sigma_2 = 4.67 \times 10^{-7}$, which is smaller than the value of the linear fit. The F -test method as discussed by Pringle (1975) was used to estimate to what extent the statistical significance is improved between the linear fit and the linear-plus-sinusoidal fit. The statistic parameter λ is corrected to be

$$\lambda = \frac{(\sigma_1^2 - \sigma_2^2)/2}{\sigma_2^2/(n - 4)}. \quad (4)$$

In this equation, n is the number of eclipse times. We obtained $F(2, 184) = 19.5$, indicating that the statistical significance of the linear-plus-sinusoidal fit with respect to the linear fit is more than the 99.99% level. The best fitting curve for the linear-plus-sinusoidal terms is displayed in the upper panel of Figure 5. The linear term of Equation (3) represents the revision on the initial linear ephemeris (Equation 1). When the linear term was removed, the $(O - C)_2$ values are displayed in the middle panel of Figure 5. A 22.8 yr cyclic modulation with an amplitude of 0.00035 days can be seen. The residuals from Equation (3) are shown in the lower panel of Figure 5, where no regular changes can be subtracted.

4. Discussion

4.1. The cyclic orbital period variation

Based on the investigation of the $O - C$ diagram, we found that the orbital period of LX Ser shows a cyclic modulation with a period of $P_3 = 22.8$ yr and an amplitude of

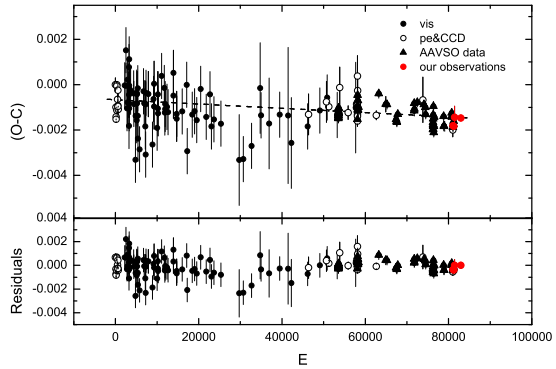


Fig. 3.— The $O - C$ diagram of LX Ser. Upper panel shows the linear fit of the $O - C$ curve. Lower panel displays the residuals. "Vis" represents the visual data, "pe" refers to the photoelectric data, and "CCD" displays the CCD data.

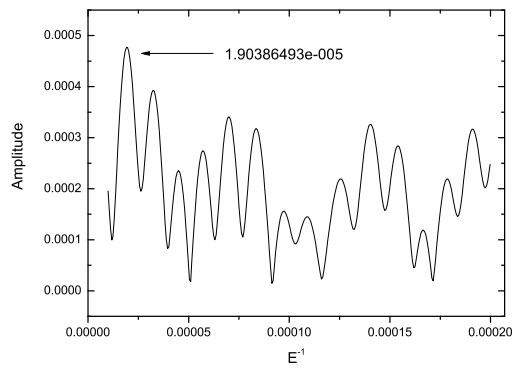


Fig. 4.— The fourier spectrum for the orbital period variation.

Table 3: All available eclipse times of LX Ser

HJD 2400000+	BJD 2400000+	Errors	Method	Cycle	O-C	(O-C) ₂ ^a	(O-C) ₃ ^b	References
44293.02430	44293.02487	0.00030	pe	0	0	0.00067	0.00082	Horne 1980
44312.98580	44312.98637	–	pe	126	-0.00100	-0.00031	-0.00017	Africano & Klimke 1981
44316.94620	44316.94677	–	pe	151	-0.00141	-0.00072	-0.00058	Africano & Klimke 1981
44320.90690	44320.90747	–	pe	176	-0.00152	-0.00083	-0.00069	Africano & Klimke 1981
44343.72270	44343.72327	–	pe	320	0.00000	0.00068	0.00081	Africano & Klimke 1981
44344.83060	44344.83117	–	pe	327	-0.00113	-0.00044	-0.00031	Africano & Klimke 1981
44346.89130	44346.89187	–	pe	340	-0.00005	0.00063	0.00076	Africano & Klimke 1981
44372.71520	44372.71576	–	pe	503	-0.00065	0.00003	0.00016	Africano & Klimke 1981
44384.75580	44384.75636	0.000050	pe	579	-0.00092	-0.00023	-0.00011	Young et al. 1981
44384.91420	44384.91476	0.000030	pe	580	-0.00095	-0.00026	-0.00014	Young et al. 1981
44385.86550	44385.86606	0.000030	pe	586	-0.00025	0.00043	0.00056	Young et al. 1981
44396.79650	44396.79706	–	pe	655	-0.00109	-0.00040	-0.00028	Africano & Klimke 1981
44644.58600	44644.58656	–	vis	2219	-0.00003	0.00067	0.00073	BBSAG 53
44691.48200	44691.48255	–	vis	2515	-0.00005	0.00065	0.00070	BBSAG 53
44691.64200	44691.64255	–	vis	2516	0.00152	0.00222	0.00228	BBSAG 53
44731.40600	44731.40655	–	vis	2767	-0.00104	-0.00033	-0.00028	BBSAG 54
44755.48800	44755.48855	–	vis	2919	-0.00078	-0.00007	-0.00002	BBSAG 54
44755.48900	44755.48955	–	vis	2919	0.00022	0.00092	0.00097	BBSAG 54
44808.40600	44808.40656	–	vis	3253	0.00077	0.00148	0.00151	BBSAG 56
44809.35400	44809.35456	–	vis	3259	-0.00182	-0.00110	-0.00107	BBSAG 56
44809.35500	44809.35556	–	vis	3259	-0.00082	-0.00010	-0.00007	BBSAG 56
44811.41500	44811.41556	–	vis	3272	-0.00044	0.00026	0.00030	BBSAG 56
44812.36500	44812.36556	–	vis	3278	-0.00104	-0.00032	-0.00029	BBSAG 56
44812.36600	44812.36656	–	vis	3278	-0.00004	0.00067	0.00070	BBSAG 56
44817.43700	44817.43756	–	vis	3310	0.00112	0.00183	0.00186	BBSAG 56
44848.33000	44848.33056	–	vis	3505	-0.00022	0.00049	0.00052	BBSAG 56
44869.24300	44869.24356	–	vis	3637	-0.00031	0.00040	0.00043	BBSAG 56
44987.59200	44987.59256	–	vis	4384	-0.00039	0.00033	0.00033	BBSAG 58
44994.72100	44994.72156	–	vis	4429	-0.00085	-0.00012	-0.00012	BBSAG 58
45053.49700	45053.49756	–	vis	4800	-0.00331	-0.00258	-0.00258	BBSAG 59
45061.57900	45061.57956	–	vis	4851	-0.00137	-0.00064	-0.00064	BBSAG 60
45101.50500	45101.50556	–	vis	5103	-0.00036	0.00037	0.00036	BBSAG 61
45104.51400	45104.51456	–	vis	5122	-0.00157	-0.00084	-0.00085	BBSAG 60
45114.49600	45114.49656	–	vis	5185	-0.00082	-0.00009	-0.00010	BBSAG 61
45115.44700	45115.44756	–	vis	5191	-0.00042	0.00031	0.00030	BBSAG 60
45115.44700	45115.44756	–	vis	5191	-0.00042	0.00031	0.00030	BBSAG 60
45139.52900	45139.52956	–	vis	5343	-0.00016	0.00057	0.00055	BBSAG 61
45142.53800	45142.53856	–	vis	5362	-0.00137	-0.00063	-0.00065	BBSAG 61
45148.39900	45148.39956	–	vis	5399	-0.00238	-0.00164	-0.00166	BBSAG 61
45208.28600	45208.28657	–	vis	5777	-0.00285	-0.00211	-0.00213	BBSAG 62
45358.64100	45358.64157	–	vis	6726	-0.00029	0.00045	0.00041	BBSAG 64
45385.57400	45385.57457	–	vis	6896	-0.00082	-0.00007	-0.00011	BBSAG 65
45432.46900	45432.46957	–	vis	7192	-0.00184	-0.00109	-0.00113	BBSAG 66
45432.47000	45432.47057	–	vis	7192	-0.00084	-0.00008	-0.00013	BBSAG 66
45439.44100	45439.44157	–	vis	7236	-0.00087	-0.00011	-0.00016	BBSAG 66
45442.44900	45442.44957	–	vis	7255	-0.00308	-0.00233	-0.00237	BBSAG 66
45459.40400	45459.40457	–	vis	7362	-0.00036	0.00038	0.00034	BBSAG 66
45548.44300	45548.44358	–	vis	7924	-0.00041	0.00034	0.00029	BBSAG 68
45548.44300	45548.44358	–	vis	7924	-0.00041	0.00034	0.00029	BBSAG 68
45701.64500	45701.64559	–	vis	8891	-0.00264	-0.00187	-0.00192	BBSAG 70
45741.57200	45741.57259	–	vis	9143	-0.00063	0.00013	0.00008	BBSAG 71
45766.60400	45766.60459	–	vis	9301	-0.00096	-0.00019	-0.00024	BBSAG 71
45766.60500	45766.60559	–	vis	9301	0.00004	0.00080	0.00075	BBSAG 71
45879.40700	45879.40759	–	vis	10013	-0.00190	-0.00112	-0.00117	BBSAG 72
45906.34200	45906.34259	–	vis	10183	-0.00042	0.00035	0.00030	BBSAG 73
45908.40100	45908.40159	–	vis	10196	-0.00105	-0.00027	-0.00032	BBSAG 73
45911.41100	45911.41159	–	vis	10215	-0.00126	-0.00048	-0.00053	BBSAG 73
46046.71400	46046.71460	–	vis	11069	0.00039	0.00117	0.00112	BBSAG 75
46154.60600	46154.60660	–	vis	11750	-0.00014	0.00064	0.00061	BBSAG 76

Table 3: — continued

HJD 2400000+	BJD 2400000+	Errors	Method	Cycle	O-C	$(O-C)_2^a$	$(O-C)_3^b$	References
46175.51800	46175.51860	—	vis	11882	-0.00123	-0.00043	-0.00047	BBSAG 76
46183.44000	46183.44060	—	vis	11932	-0.00086	-0.00006	-0.00009	BBSAG 77
46186.45000	46186.45060	—	vis	11951	-0.00107	-0.00027	-0.00031	BBSAG 77
46252.35800	46252.35862	—	vis	12367	-0.00098	-0.00018	-0.00021	BBSAG 77
46296.40200	46296.40262	—	vis	12645	-0.00121	-0.00041	-0.00043	BBSAG 78
46497.61200	46497.61262	—	vis	13915	-0.00048	0.00032	0.00033	BBSAG 79
46497.61300	46497.61362	—	vis	13915	0.00052	0.00132	0.00133	BBSAG 79
46622.45600	46622.45663	—	vis	14703	-0.00129	-0.00047	-0.00045	BBSAG 80
46625.46600	46625.46663	—	vis	14722	-0.00150	-0.00068	-0.00066	BBSAG 81
46831.58700	46831.58764	—	vis	16023	-0.00118	-0.00034	-0.00029	BBSAG 82
47003.32900	47003.32964	—	vis	17107	-0.00001	0.00083	0.00092	BBSAG 84
47023.44700	47023.44764	—	vis	17234	-0.00293	-0.00208	-0.00199	BBSAG 85
47212.61700	47212.61765	—	vis	18428	-0.00132	-0.00046	-0.00033	BBSAG 87
47304.50800	47304.50866	—	vis	19008	-0.00117	-0.00031	-0.00015	BBSAG 88
47383.40700	47383.40766	—	vis	19506	-0.00156	-0.00069	-0.00052	BBSAG 89
47535.66200	47535.66266	—	vis	20467	-0.00019	0.00068	0.00089	BBSAG 90
47746.37600	47746.37665	—	vis	21797	-0.00142	-0.00053	-0.00027	BBSAG 92
47890.70900	47890.70965	—	vis	22708	-0.00042	0.00046	0.00076	BBSAG 93
47942.51500	47942.51566	—	vis	23035	-0.00184	-0.00094	-0.00063	BBSAG 94
48039.47600	48039.47666	—	vis	23647	-0.00153	-0.00062	-0.00029	BBSAG 95
48306.59300	48306.59367	0.00100	vis	25333	-0.00172	-0.00080	-0.00041	BBSAG 97
49004.64500	49004.64566	0.00200	vis	29739	-0.00332	-0.00236	-0.00185	BBSAG 103
49158.48300	49158.48366	0.00100	vis	30710	-0.00328	-0.00231	-0.00178	BBSAG 104
49475.50700	49475.50767	—	vis	32711	-0.00270	-0.00171	-0.00116	BBSAG 106
49799.50400	49799.50469	0.00200	vis	34756	-0.00015	0.00085	0.00140	BBSAG 108
49836.57600	49836.57669	0.00100	vis	34990	-0.00135	-0.00034	0.00020	BBSAG 109
50139.65700	50139.65771	0.00200	vis	36903	-0.00171	-0.00068	-0.00015	BBSAG 111
50539.54100	50539.54172	0.00100	vis	39427	-0.00132	-0.00026	0.00020	BBSAG 114
50864.48600	50864.48675	0.00300	vis	41478	-0.00136	-0.00028	0.00011	BBSAG 117
50988.37900	50988.37975	0.00200	vis	42260	-0.00257	-0.00149	-0.00111	BBSAG 118
51603.57310	51603.57388	—	vis	46143	-0.00184	-0.00072	-0.00051	BRNO 32
51641.43900	51641.43978	0.00090	ccd	46382	-0.00131	-0.00019	0.00001	OEJV 74
52072.53400	52072.53477	—	vis	49103	-0.00114	0	0.00007	BBSAG 125
52320.63969	52320.64046	0.00090	ccd	50669	-0.00075	0.00040	0.00040	OEJV 74
52348.52400	52348.52476	—	vis	50845	-0.00057	0.00059	0.00059	BBSAG 127
52410.47070	52410.47146	0.00020	pe	51236	-0.00097	0.00018	0.00017	Agerer & Hubscher 2003
52730.50400	52730.50475	0.00100	vis	53256	-0.00134	-0.00015	-0.00025	Diethelm 2003
52777.87530	52777.87605	0.00008	pe	53555	-0.00135	-0.00016	-0.00027	This paper
52778.82581	52778.82656	0.00010	pe	53561	-0.00144	-0.00025	-0.00036	This paper
52779.77639	52779.77714	0.00008	pe	53567	-0.00145	-0.00026	-0.00037	This paper
52779.93490	52779.93565	0.00012	pe	53568	-0.00138	-0.00019	-0.00030	This paper
52780.72718	52780.72793	0.00015	pe	53573	-0.00126	-0.00007	-0.00018	This paper
52780.88538	52780.88613	0.00013	pe	53574	-0.00149	-0.00030	-0.00041	This paper
52781.83613	52781.83688	0.00012	pe	53580	-0.00134	-0.00015	-0.00026	This paper
52782.78677	52782.78752	0.00012	pe	53586	-0.00129	-0.00010	-0.00021	This paper
52782.94532	52782.94607	0.00013	pe	53587	-0.00117	0.00001	-0.00009	This paper
52783.73740	52783.73815	0.00009	pe	53592	-0.00126	-0.00007	-0.00018	This paper
52786.74781	52786.74856	0.00013	pe	53611	-0.00106	0.00012	0.00001	This paper
52786.90609	52786.90684	0.00009	pe	53612	-0.00122	-0.00003	-0.00014	This paper
52787.85687	52787.85762	0.00010	pe	53618	-0.00103	0.00015	0.00004	This paper
52828.41650	52828.41725	0.00090	ccd	53874	-0.00012	0.00106	0.00094	Zejda 2004
53146.23100	53146.23174	0.00030	ccd	55880	-0.00123	-0.00002	-0.00020	Krajci 2005
53436.63800	53436.63873	0.00200	vis	57713	-0.00101	0.00021	-0.00001	OEJV 3
53465.63130	53465.63203	0.00030	ccd	57896	-0.00086	0.00036	0.00013	Zejda et al. 2006
53498.26840	53498.26913	—	ccd	58102	-0.00085	0.00037	0.00013	VSOLJ 44
53500.48638	53500.48711	0.00011	pe	58116	-0.00093	0.00029	0.00005	This paper
53500.80300	53500.80373	0.00020	ccd	58118	-0.00118	0.00004	-0.00019	Krajci 2006
53500.96130	53500.96203	0.00030	ccd	58119	-0.00131	-0.00008	-0.00032	Krajci 2006

Table 3: — continued

HJD 2400000+	BJD 2400000+	Errors	Method	Cycle	O-C	$(O-C)_2^a$	$(O-C)_3^b$	References
53501.75400	53501.75473	0.00060	ccd	58124	-0.00077	0.00045	0.00021	Krajci 2006
53501.91160	53501.91233	0.00020	ccd	58125	-0.00160	-0.00037	-0.00061	Krajci 2006
53502.54540	53502.54613	0.00031	pe	58129	-0.00153	-0.00030	-0.00054	This paper
53504.76360	53504.76433	0.00020	ccd	58143	-0.00139	-0.00016	-0.00040	Krajci 2006
53504.92380	53504.92453	0.00090	ccd	58144	0.00038	0.00160	0.00136	Krajci 2006
53506.50728	53506.50801	0.00033	pe	58154	-0.00046	0.00076	0.00052	This paper
53510.46830	53510.46903	0.00050	ccd	58179	-0.00026	0.00096	0.00073	Hubscher et al. 2005
53514.42838	53514.42911	0.00037	pe	58204	-0.00099	0.00023	0.00000	This paper
53516.48800	53516.48873	0.00035	pe	58217	-0.00099	0.00023	0.00000	This paper
53519.49811	53519.49884	0.00042	pe	58236	-0.00110	0.00012	-0.00011	This paper
53521.39970	53521.40043	0.00039	pe	58248	-0.00070	0.00052	0.00028	This paper
53521.55769	53521.55842	0.00040	pe	58249	-0.00114	0.00008	-0.00015	This paper
53541.52033	53541.52106	0.00012	pe	58375	-0.00100	0.00023	-0.00001	This paper
54218.34361	54218.34434	0.00020	ccd	62647	-0.00135	-0.00008	-0.00034	OEJV 107
54316.41428	54316.41502	0.00008	ccd	63266	-0.00040	0.00087	0.00061	This paper
54580.52079	54580.52153	0.00034	ccd	64933	-0.00086	0.00043	0.00018	This paper
54628.52582	54628.52656	0.00013	ccd	65236	-0.00088	0.00041	0.00017	This paper
54976.44292	54976.44368	0.00014	ccd	67432	-0.00153	-0.00021	-0.00040	This paper
54994.50413	54994.50489	0.00006	ccd	67546	-0.00162	-0.00030	-0.00049	This paper
55001.47512	55001.47588	0.00007	ccd	67590	-0.00166	-0.00034	-0.00053	This paper
55037.43966	55037.44042	0.00017	ccd	67817	-0.00130	0.00001	-0.00016	This paper
55662.45633	55662.45711	0.00016	ccd	71762	-0.00082	0.00053	0.00047	This paper
55663.40660	55663.40738	0.00022	ccd	71768	-0.00115	0.00020	0.00015	This paper
55672.43733	55672.43811	0.00016	ccd	71825	-0.00107	0.00028	0.00023	This paper
55778.42896	55778.42974	0.00011	ccd	72494	-0.00078	0.00058	0.00055	This paper
55988.66900	55988.66978	0.00100	ccd	73821	-0.00067	0.00070	0.00072	OEJV 147
56028.43535	56028.43613	0.00010	ccd	74072	-0.00088	0.00050	0.00053	This paper
56088.48114	56088.48192	0.00009	ccd	74451	-0.00100	0.00038	0.00042	This paper
56101.63073	56101.63151	0.00012	ccd	74534	-0.00131	0.00007	0.00012	This paper
56378.88725	56378.88804	0.00014	ccd	76284	-0.00166	-0.00026	-0.00014	This paper
56381.89715	56381.89794	0.00019	ccd	76303	-0.00198	-0.00058	-0.00046	This paper
56383.79856	56383.79935	0.00029	ccd	76315	-0.00176	-0.00036	-0.00024	This paper
56384.43209	56384.43288	0.00015	ccd	76319	-0.00196	-0.00056	-0.00044	This paper
56384.59069	56384.59148	0.00015	ccd	76320	-0.00179	-0.00039	-0.00027	This paper
56384.74908	56384.74987	0.00016	ccd	76321	-0.00183	-0.00043	-0.00031	This paper
56385.85843	56385.85922	0.00020	ccd	76328	-0.00151	-0.00011	0.00000	This paper
56386.80920	56386.80999	0.00017	ccd	76334	-0.00133	0.00006	0.00018	This paper
56389.50214	56389.50293	0.00011	ccd	76351	-0.00175	-0.00035	-0.00023	This paper
56389.66136	56389.66215	0.00021	ccd	76352	-0.00096	0.00043	0.00055	This paper
56403.44384	56403.44463	0.00008	ccd	76439	-0.00211	-0.00071	-0.00058	This paper
56410.41514	56410.41593	0.00016	ccd	76483	-0.00184	-0.00044	-0.00031	This paper
56427.68469	56427.68548	0.00020	ccd	76592	-0.00143	-0.00002	0.00009	This paper
56782.41510	56782.41588	0.00006	ccd	78831	-0.00140	0.00002	0.00022	This paper
56792.39590	56792.39668	0.00020	ccd	78894	-0.00184	-0.00041	-0.00021	This paper
56798.41636	56798.41714	0.00006	ccd	78932	-0.00182	-0.00039	-0.00019	This paper
57091.67550	57091.67627	0.00007	ccd	80783	-0.00125	0.00018	0.00044	This paper
57094.68559	57094.68636	0.00021	ccd	80802	-0.00137	0.00007	0.00033	This paper
57097.69575	57097.69652	0.00005	ccd	80821	-0.00143	0.00001	0.00027	This paper
57132.39190	57132.39267	0.00030	pe	81040	-0.00200	-0.00055	-0.00029	Hubscher 2016
57134.45164	57134.45241	0.00004	ccd	81053	-0.00188	-0.00043	-0.00017	This paper
57135.40230	57135.40307	0.00020	pe	81059	-0.00182	-0.00037	-0.00011	Hubscher 2016
57137.30350	57137.30427	0.00007	ccd	81071	-0.00181	-0.00036	-0.00010	This paper
57159.48411	57159.48488	0.00005	ccd	81211	-0.00175	-0.00030	-0.00003	This paper
57163.44506	57163.44583	0.00013	ccd	81236	-0.00161	-0.00016	0.00010	This paper
57173.26766	57173.26843	0.00015	ccd	81298	-0.00183	-0.00038	-0.00011	This paper
57200.04314	57200.04391	0.00049	ccd	81467	-0.00144	0	0.00028	This paper
57439.27618	57439.27695	0.00004	ccd	82977	-0.00147	0	0.00029	This paper

^a (O-C)₂ means the residuals for Equation (2), ^b (O-C)₃ means the residuals for Equation (3)

$A_3 = 0.00035$ days. The cyclic change of the $O - C$ diagram can be explained either by the Applegate mechanism (Applegate 1992) due to the magnetic activity of the red dwarf component or by the light travel time effect due to a tertiary companion.

The Applegate mechanism was proposed according to the conclusion determined by Hall (1989) who analyzed the orbital period variations of 101 Algols. Hall (1989) found that all the binary systems which show cyclic period changes have late spectral type secondary components. However, a recently statistical study by Liao & Qian (2010) reveals that the percentages for both late type and early type binary systems that exhibit cyclic orbital period changes are similar, and they concluded that the cyclic oscillation is most likely caused by the light travel time effect via the presence of a third body.

According to Applegate mechanism, solar-like magnetic cycles would result in shape changes of the low-mass components, thus redistributing the angular momentum within the interior of the star. Then, the oblateness is changed, causing a change of the stellar quadrupole moment which consequently leads to the variation of orbital period. Using the equation

$$\frac{\Delta P}{P} = 2\pi \frac{O - C}{P_{mod}}, \quad (5)$$

where $(O - C)$ and P_{mod} are the amplitude and modulation period of the cyclic oscillation of the orbital period. The fractional period change $\frac{\Delta P}{P}$ was determined to be 2.67×10^{-7} . By considering a typical mass of $M_1 = 0.6 M_\odot$ for the primary white dwarf of LX Ser, the mass of the secondary red dwarf can be calculated to be $M_2 = q \times M_1 = 0.3 M_\odot$ (the mass ratio q is 0.5 based on the result of Marin et al. 2007). The radius of the secondary red dwarf was estimated to be $0.38 R_\odot$ based on Cox (2000), the binary separation $a = 1.19 R_\odot$ can be derived using $M_1 + M_2 = 0.0134a^3/P^2$. Then, according to the equation

$$\frac{\Delta P}{P} = -9 \left(\frac{R_2}{a} \right)^2 \frac{\Delta Q}{M_2 R_2^2}, \quad (6)$$

we determined the variation of the quadrupole moment of the red dwarf to be $\Delta Q = -1.21 \times 10^{47}$ g cm². The secondary component of LX Ser may be a full convective star, we can use the same method that Brinkworth et al. (2006) used to calculate the energy required to produce the cyclic modulation of LX Ser. We split the whole star into an inner core (denotes as 1) and an outer shell (denotes as 2). By employing the Lane-Emden equation for an $n = 1.5$ polytrope, different shell mass versus the required energy ΔE can be calculated and is displayed in Figure 6. The minimum value of the required energy is achieved to be $\Delta E_{min} = 8.95 \times 10^{40}$ erg when $M_s = 0.224 M_\odot$. Assuming that the temperature of $T_2 = 3500$ K, the total radiated energy of the secondary red dwarf over the whole modulation period is also shown in Figure 6. Obviously, the Applegate mechanism has difficulty to explain the cyclic oscillation in the $O - C$ diagram.

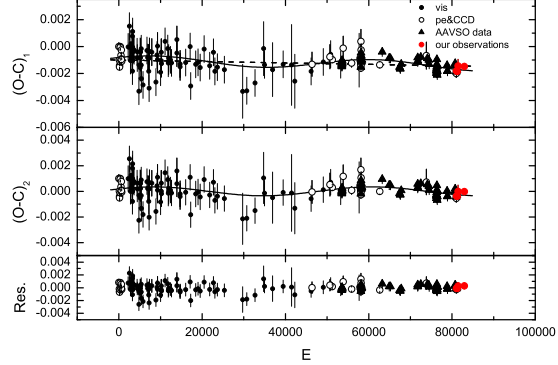


Fig. 5.— The best fitting curve for the linear-plus-sinusoidal terms of LX Ser.

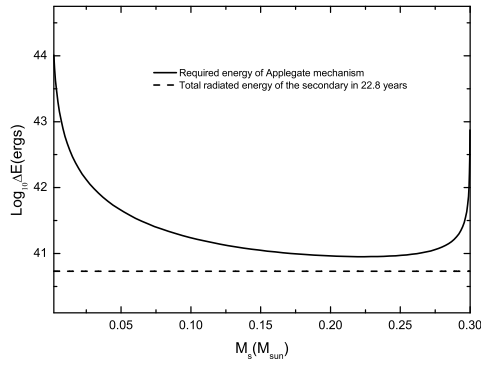


Fig. 6.— The required energy ΔE versus different shell mass. The lowest value of required energy is 8.95×10^{40} erg at a shell-mass of $0.224 M_{\odot}$.

Therefore, like many other CVs, DQ Her (Dai & Qian 2009), UZ For (Potter et al. 2011), AM Her (Dai et al. 2013), the plausible explanation of the cyclic modulation is the light travel time effect. Using the equation

$$f(m) = \frac{(m_3 \sin i)^3}{(m_1 + m_2 + m_3)^2} = \frac{4\pi}{GP_3^2} \times (a_{12} \sin i)^3, \quad (7)$$

the mass function $f(m) = 4.29(\pm 2.94) \times 10^{-7} M_\odot$ and the mass of the third companion $M_3 \sin i' = 0.0071(\pm 0.0027) M_\odot = 7.4(\pm 2.8) M_{Jup}$ were computed. Simulations by Bonnell & Bate (1994) and Holman & Wiegert (1999) exhibit that circumbinary planets have stable orbits and are most possibly coplanar with the central eclipsing host systems. Considering the orbital inclination of LX Ser $i = 79^\circ.0$, the mass of the third body is derived to be $M_3 = 0.0072(\pm 0.0027) M_\odot = 7.5(\pm 2.8) M_{Jup}$ with a separation of $9.12(\pm 4.03)$ AU. Based on the theoretical analysis (e.g., Chabrier & Baraffe 2000; Burrows et al. 2001), the upper limit mass of a planet is about $0.0140 M_\odot \sim 14.6 M_{Jup}$, the third companion is most likely to be a giant planet.

4.2. The stability of the possible planet

In this subsection, we discussed the stability of the possible planet. As the mass of LX Ser is much larger than the outer planet, we can ignore it when considering the evolution of the inner CV. The logarithmically differentiating of semi-major axis of LX Ser with respect to time gives

$$\frac{\dot{a}}{a} = \frac{2\dot{J}_{orb}}{J_{orb}} + \frac{2(-\dot{M}_2)}{M_2} \left(1 - \frac{M_2}{M_1}\right). \quad (8)$$

When assuming a constant angular momentum, the period of the orbit increases, which may impact the stability of the outer planet. However, there are many factors that influence the orbital angular momentum in close binary systems, especially in a CV system. The dominant angular momentum losses (AML) mechanism in long-period systems ($P_{orb} \geq 3\text{hrs}$) is "magnetic braking", whereas short period CVs ($P_{orb} \leq 2\text{hrs}$) are assumed to be driven by AML associated with the emission of "gravitational radiation" (Knigge & Baraffe 2011). Apart from the two major factors, we should also consider mass transfer, mass accretion, common-envelope evolution, wind accretion, tidal evolution and many other factors (Hurley & Tout 2002). These factors are important in the orbital evolution of CVs. We adopted the algorithm illustrated in Hurley & Tout (2002) and did a simulation with $M_1 = 0.6M_\odot$, $M_2 = 0.3M_\odot$, $P = 0.^d158$, $e = 0$, $z = 0.02$, where e is the eccentricity and z is the metallicity. The evolutions of the masses of the two components, orbital period of LX Ser are shown in Figure 7.

With multiple factors considered, we can see that the mass changes of the two components occur at different time and speed, which is mainly caused by wind accretion. Besides, the orbit of LX Ser contracts at the beginning of the evolution, mainly caused by gravitational mechanism. With the evolution of the secondary component, the period of the system is growing at a slow speed. Even at the universe timescale, the period is at most $0.^d16$, without much difference with its initial period. Therefore, while considering the orbital evolution of the outer planet, we can regard the inner CV as a particle with decreasing mass. The outer planet will drift slowly away from the inner CV, the system remains stable.

Now we consider whether the existence of a planet with the characteristics derived in the previous subsection is compatible with the evolution of LX Ser from a wide orbit binary to a CV. Similar consideration has been carried out in recent work of Bruch (2014). If the planet can survive the common envelope phase of the binary, the separation of the planet from the binary should be larger than the radius R_{CE} of the common envelope. R_{CE} is approximated by the radius R_{max} of progenitor star which evolves to be a giant star with its core mass equal to the mass of the white dwarf. According to Joss et al. (1987), the relation between the core mass and the radius is

$$R \approx \frac{3.7 \times 10^3 \mu^4}{1 + \mu^3 + 1.75\mu^4} R_{\odot}. \quad (9)$$

With the mass of the white dwarf adopted to be $0.6 M_{\odot}$, we can estimate the radius of the giant star in the common envelope phase to be $R_{\text{max}} = 1.53$ AU. As the mass loss of the primary star during the common envelope phase leads to a widening of the planetary orbit, we should compare the radius of the progenitor star to the original separation of the planet from the inner binary. According to Zhao et al. (2012), the initial-final-mass-relation for the white dwarf is

$$M_f = (0.452 \pm 0.045) + (0.073 \pm 0.019)M_i. \quad (10)$$

Where M_i is the initial mass of the white dwarf, i.e., the mass of the progenitor star, M_f is the mass of the white dwarf after the common envelope phase. As M_f here is $0.6 M_{\odot}$, the mass of the progenitor is about $M_{\text{prog}} = 2.03 M_{\odot}$. We assume that the orbital angular momentum of the planet is constant during the common envelope phase and the mass of the secondary star changes little. So,

$$m_p \frac{M_{\text{prog}} + M_2}{M_{\text{prog}} + M_2 + m_p} \sqrt{(M_{\text{prog}} + M_2)a_i} = m_p \frac{M_1 + M_2}{M_1 + M_2 + m_p} \sqrt{(M_1 + M_2)a_f}, \quad (11)$$

where a_i is the original semi-major axis of the planet and a_f is the current semi-major axis which is determined to be $a_f = 9.12 \pm 4.03$ AU. At the lower limit, $a_i \simeq 1.97$ AU, at the upper limit, $a_i \simeq 5.08$ AU, therefore, $a_i > R_{\text{max}}$ even at the lower limit. So the planet can

survive the common envelope phase and have no conflicts with the evolution of the binary system.

5. Conclusions

The CV LX Ser was observed on four nights using the 1.0 m Cassegrain telescope at Weihai Observatory of Shandong University, and four new eclipsing times with high precision were determined. Based on the data from AAVSO International Data base, 58 eclipse times were redetermined. Further more, combining all the eclipse times from O-C Gateway, we analyzed the $O - C$ behavior of LX Ser. The $O - C$ diagram shows a cyclic variation with an amplitude of 0.00035 days and period of 22.8 yr.

For the cyclic variation in the $O - C$ diagram, both of the Applegate mechanism and the light travel time effect are considered. The energy required to produce the cyclic modulation of LX Ser was calculated, we found that the minimum value of the required energy is nearly two times of the total radiated energy of the secondary red dwarf over the whole modulation period. Therefore, the Applegate mechanism is too feeble to explain the cyclic modulation. According to the investigation of the light travel time effect, a giant planet with a mass of $7.5 M_{Jup}$ at a distance of 9.12 AU was explored. Exoplanets can survive almost anywhere based on the analysis during the last 24 years (e.g., Wolszczan & Frail 1992; Silvotti et al. 2007; Qian et al. 2009, 2012). The existence of the giant planet orbiting the CV LX Ser is reasonable. By considering all the factors, we analyzed the the stability of the multiple systems and we found that the outer planet will move slowly away from the centre eclipsing CV and the system will stay stable. We also considered whether the existence of the giant planet is compatible with the evolution of LX Ser from a wide orbit binary to a CV and we determined that the planet can survive the common envelope phase and have no conflicts with the evolution of the binary system. In the future, more eclipse times with high precision are needed to confirm the possibility of the giant planet.

This work is partly supported by the National Natural Science Foundation of China and the Chinese Academy of Sciences joint fund on astronomy (No. U1431105) and by the National Natural Science Foundation of China (No. 11333002), and by the Natural Science Foundation of Shandong Province (No. ZR2014AQ019), and by Young Scholars Program of Shandong University, Weihai (No. 2016WHLJH07), and by the Open Research Program of Key Laboratory for the Structure and Evolution of Celestial Objects (No. OP201303). The authors thanks the AAVSO International Database very much for the observations of LX Ser. The data used in this paper were contributed by worldwide observers as follows:

Bruno, Alain; Carreno, Alfonso; Cook, Michael; Darriba Martinez, Adolfo; Bubovsky, Pavol; Foster, James; Gomez, Tomas; Graham, Keith; Gualdoni, Carlo; James, Robert; Macdonald, Walter; Menzise, Kenneth; Poyner, Gary; Roe, James. Many thanks to the referee for the helpful comments and suggestions that helped to greatly improve this paper.

REFERENCES

- Agerer, Franz, Hubscher, Joachim 2003, IBVS, 5484, 1
Africano, J. L., Klimke, A. 1981, IBVS, 1969, 1
Applegate, J. H. 1992, ApJ, 385, 621
Bonnell, I. A., Bate, M. R. 1994, MNRAS, 269, L45
Burrows, A., Hubbard, W. B., Lunine, J. T., Liebert, J. 2001, RvMP, 73, 719
Brinkworth, C. S., Marsh, T. R., Dhillon, V. S., Knigge, C. 2006, MNRAS, 365, 287
Bruch, Albert 2014, A&A, 566, 101
Chabrier, G., Baraffe, I. 2000, ARA&A, 38, 337
Cox A. N., 2000, Allen's astrophysical quantities, 4th ed. Publisher: New York: AIP Press; Springer
Dai, Z. B., Qian, S. B. 2009, A&A, 503, 883
Dai, Z. B., Qian, S. B., Fernández Lajús, E. 2009, ApJ, 703, 109
Dai, Z. B., Qian, S. B., Li, L. J. 2013, ApJ, 207, 22
Diethelm, Roger 2003, IBVS, 5438, 1
Eason, E. L. E., Worden, S. P., Klimke, A., Africano, J. L. 1984, PASP, 96, 372
Eastman, Jason, Siverd, Robert, Gaudi, B. Scott 2010, PASP, 122, 935
Hall, D. S. 1989, SSRv, 50, 219
Holman, M. J., Wiegert, P. A. 1999, AJ, 117, 621
Horne, K. 1980, ApJ, 242, L167
Hu, S. M., Han, S. H., Guo, D. F., Du, J. J. 2014, RAA, 14, 719
Hubscher, Joachim 2016, IBVS, 6157, 1
Hubscher, Joachim, Paschke, Anton, Walter, Frank 2005, IBVS, 5657, 1
Hurley, J., Tout, C.-M. 2002, MNRAS, 329, 897
Joss, P. C., Rappaport, S., Lewis, W. 1987, ApJ, 319, 180.

- Knigee, C., Baraffe, I. 2011, ApJS, 194, 28
- Krajci, Tom 2005, IBVS, 5592,1
- Krajci, Tom 2006, IBVS, 5690,1
- Liao W.-P., Qian S.-B. 2010, MNRAS, 405, 1930
- Lenz, P., Breger, M. 2005, CoAst, 144, 41
- Marin, Eduardo, Shafter, A. W., Misselt, K. A. 2007, AAS, 211, 5108
- Pringle, J. E. 1975, MNRAS, 170, 633
- Potter, Stephen B., Romero-Colmenero, Encarni, Ramsay, Gavin et al. 2011, MNRAS, 416, 2202
- Qian, S. B., Han, Z. T., Fernández Lajús, E., Zhu, L. Y., Li, L. J., Liao, W. P., Zhao, E. G. 2015, ApJS, 221, 17
- Qian, S.-B., Dai, Z.-B., Liao, W.-P., Zhu, L.-Y., Liu, L., Zhao, E. G. 2009, ApJ, 706, L96
- Qian, S.-B., Liao, W.-P., Zhu, L.-Y., Dai, Z.-B., Liu, L., He, J.-J., Zhao, E.-G., Li, L.-J. 2010b, MNRAS, 401, 34
- Qian, S.-B., Liu, L., Zhu, L.-Y., Dai, Z.-B., Fernández Lajús, E., Baume, G. L. 2012, MNRAS, 422, 24
- Qian, S.-B., Liao, W.-P., Zhu, L.-Y., Dai, Z.-B. 2010a, ApJ, 708, L66
- Silvotti, R., Schuh, S., Janulis, R. et al. 2007, Nature, 449, 189
- Stepanian, J. A. 1979, IBVS, 1630, 1
- Wolszczan, A., Frail, D. A. 1992, Nature, 355, 145
- Young, P., Schneider, D. P., Shectman, S. A. 1981, ApJ, 244, 259
- Zejda, M., Mikulasek, Z., Wolf, M. 2006, IBVS, 5741, 1
- Zejda, Miloslav 2004, IBVS, 5583, 1
- Zhao, J. K., Oswalt, T. D., Willson, L. A., Wang, Q., Zhao, G. 2012, A&A, 746, 144

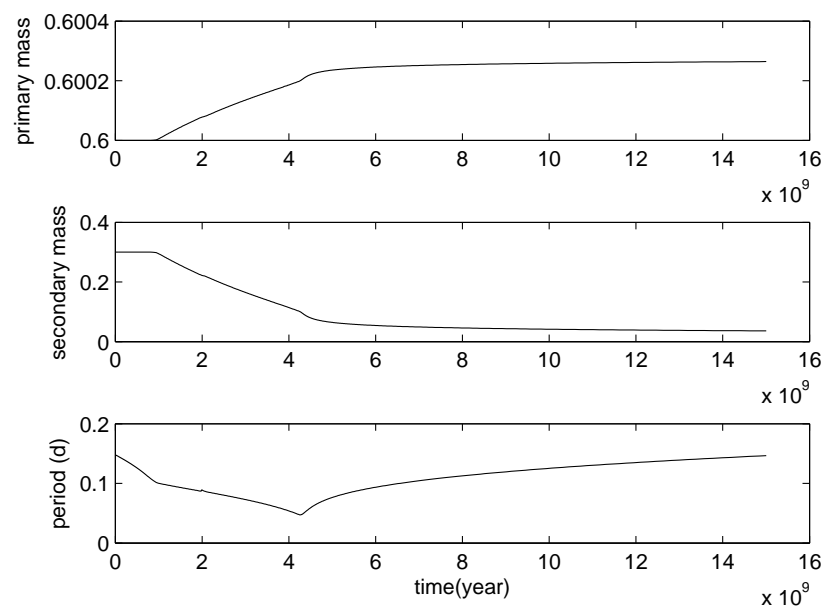


Fig. 7.— Evolution of masses of the two components and period of LX Ser.